AAC Journals.ASM.org

Antibiofilm and Membrane-Damaging Potential of Cuprous Oxide Nanoparticles against *Staphylococcus aureus* with Reduced Susceptibility to Vancomycin

Avinash Singh,[a,c] Asar Ahmed,[b] Kashi N. Prasad,[a] Sonali Khanduja,[a] Satyendra K. Singh,[a] Janmejai K. Srivastava,[c] Namdeo S. Gajbhiye[b]

Department of Microbiology, Sanjay Gandhi Postgraduate Institute of Medical Sciences, Lucknow, India[a]; Department of Chemistry, Indian Institute of Technology, Kanpur, India[b]; Amity Institute of Biotechnology, Amity University Uttar Pradesh, Lucknow, India[c]

The antimicrobial effects of copper ions and salts are well known, but the effects of cuprous oxide nanoparticles (Cu_2O-NPs) on staphylococcal biofilms have not yet been clearly revealed. The present study evaluated Cu_2O-NPs for their antibacterial and antibiofilm activities against heterogeneous vancomycin-intermediate *Staphylococcus aureus* (hVISA) and vancomycin-intermediate *S. aureus* (VISA). Nanoscaled Cu_2O, generated by solution phase technology, contained Cu_2O octahedral nanoparticles. Field emission electron microscopy demonstrated particles with sizes ranging from 100 to 150 nm. Cu_2O-NPs inhibited the growth of *S. aureus* and showed antibiofilm activity. The MICs and minimum biofilm inhibitory concentrations ranged from 625 μg/ml to 5,000 μg/ml and from 2,500 μg/ml to 10,000 μg/ml, respectively. Exposure of *S. aureus* to Cu_2O-NPs caused leakage of the cellular constituents and increased uptake of ethidium bromide and propidium iodide. Exposure also caused a significant reduction in the overall vancomycin-BODIPY (dipyrromethene boron difluoride [4,4-difluoro-4-bora-3*a*,4*a*-diaza-*s*-indacene] fluorescent dye) binding and a decrease in the viable cell count in the presence of 7.5% sodium chloride. Cu_2O-NP toxicity assessment by hemolysis assay showed no cytotoxicity at 625 to 10,000 μg/ml concentrations. The results suggest that Cu_2O-NPs exert their action by disruption of the bacterial cell membrane and can be used as effective antistaphylococcal and antibiofilm agents in diverse medical devices.

Biofilm formation, one of the defense mechanisms of *Staphylococcus aureus*, represents a structural community of bacterial cells embedded in a self-produced polymeric matrix adherent to an artificial surface (1). Biofilms can be associated with a variety of complications, the worst being the risk of bacterial and fungal infections in surgical implanted devices. Bacteria embedded in biofilms are hard to eradicate with standard antibiotics and are intrinsically resistant to host immune responses (2). *S. aureus* strains with reduced susceptibility to vancomycin, such as heterogeneous vancomycin-intermediate *Staphylococcus aureus* (hVISA) and vancomycin-intermediate *Staphylococcus aureus* (VISA), are being reported increasingly worldwide (3). The emergence of such strains is attributed to excess or irrational use of vancomycin and poor tissue penetration (4). Biofilm formation also plays an important role in the pathogenesis of staphylococcal infections, especially with prosthetic materials (5). It is presumed to be a significant initial step in the pathway to development of vancomycin resistance (6, 7). Biofilm infections are difficult to treat due to their inherent antibiotic resistance (8). Only limited numbers of antibiotics, such as daptomycin, quinupristin-dalfopristin, linezolid, and tigecycline, are active against the vancomycin-nonsusceptible *S. aureus* strains (9). Interestingly, daptomycin nonsusceptibility is also being reported for some hVISA and VISA isolates (10, 11). Despite antimicrobial therapy, the morbidity and mortality associated with these bacterial infections remain high (12). As resistance in bacteria to available antibiotics is increasing, new strategies are, therefore, warranted to identify and develop the next generation of drugs or agents to treat such infections. The use of several nanomaterials in medical science and technological areas is flourishing, while researchers are exploring potential applications in biosensors, biomaterials, tissue engineering, DNA modification, and drug-delivery systems (13). Recent advances in the field of nanotechnology, particularly the ability to prepare highly ordered nanoparticles of any size and shape, have led to the development of new biocidal agents. Previous studies indicated that nanoparticulate formulations might be used as effective bactericidal materials (14). It was reported that metal nanoparticles (Ag, Cu, CuO, Au) exhibited a wide spectrum of antimicrobial activities against different microorganisms, including fungi and Gram-positive and Gram-negative bacteria (15).

Due to their unique properties, copper oxide nanomaterials have attracted more attention than those of other metal oxides. Cuprous oxide (Cu_2O) is a p-type semiconductor with a direct band gap of 2.17 eV. In recent years, there has been growing interest in synthesizing Cu_2O nanoparticles (Cu_2O-NPs) as antibacterial agents against Gram-positive bacteria due to their rapid availability and properties similar to those of other expensive noble metals, including silver and gold (16). Recently, Huang and others (17) demonstrated that Cu_2O nanoparticles exhibit excel-

Received 18 June 2015 **Returned for modification** 20 July 2015
Accepted 14 August 2015
Accepted manuscript posted online 24 August 2015
Citation Singh A, Ahmed A, Prasad KN, Khanduja S, Singh SK, Srivastava JK, Gajbhiye NS. 2015. Antibiofilm and membrane-damaging potential of cuprous oxide nanoparticles against *Staphylococcus aureus* with reduced susceptibility to vancomycin. Antimicrob Agents Chemother 59:6882–6890. doi:10.1128/AAC.01440-15.

Address correspondence to Kashi N. Prasad, kashinprasad@gmail.com.

lent biocidal action against *S. aureus*. Moreover, antibacterial activity against *Escherichia coli* has also been reported (4, 18).

Several techniques, such as thermal reduction, the capping agent method, sonochemical reduction, metal vapor synthesis, the microemulsion technique, laser irradiation, and induced radiation, can be used to prepare copper nanoparticles (15). Most of these techniques require organic solvents and a high temperature and involve multistep sample preparation processes (19). However, the solution phase technique is cheaper, and it does not require any organic compound or surfactant or a high temperature for Cu_2O-NP synthesis (20). Chemically and physically, Cu_2O-NPs can be prepared with extremely high surface areas and unusual crystal morphologies, which act predominantly as valuable antistaphylococcal agents (2). Previously, it was observed that copper (Cu)-containing nanoparticles (Cu metal, Cu, CuO) caused cell membrane damage, depending on both the chemical composition (metal versus oxide) and surface area (21). Their activity against hVISA and VISA isolates has not been reported so far. Therefore, the present study was designed to investigate the antibiofilm activity and possible mode of action of Cu_2O-NPs synthesized by the solution phase method against hVISA and VISA strains.

MATERIALS AND METHODS

Bacterial strains. Five bacterial strains, *S. aureus* ATCC 29213, Mu3 (hVISA), Mu50 (VISA), and St1745 and B10760 (clinical isolates of hVISA), were used in this study. The cultures were stored at −80°C in brain heart infusion broth (BHIB) (HiMedia, Mumbai, India) containing 20% glycerol (vol/vol) until further use.

Synthesis of Cu_2O-NPs. Cu_2O-NPs were synthesized by the solution phase method as follows: 0.5 g of $CuSO_4 \cdot 5H_2O$ (2 mmol) and 0.361 g of D-glucose (2 mmol) were completely dissolved in 100 ml of double-distilled water in a 250-ml round-bottom flask with constant argon gas flow and magnetic stirring. After 15 to 20 min of stirring, 2 ml of 10 M NaOH was added in a drop-wise manner, with the help of a dropping funnel, into the solution, and a blue-colored solution of $Cu(OH)_2$ was soon produced. After a further 30 min of stirring, 3 ml of 2 M hydrazine hydrate ($N_2H_4 \cdot H_2O$) solution was added drop by drop to this solution; the color of the solution gradually changed from blue to brick red. The solution was stirred until the cuprous hydroxide [$Cu(OH)_2$] precipitates were completely reduced by the hydrazine hydrate to brick red. The brick red precipitates were collected, washed with methanol (high-performance liquid chromatography [HPLC]-grade) several times, centrifuged, and dried in a vacuum oven at 60°C for 3 h.

Antimicrobial susceptibility assay and determination of MICs. MICs were determined for all of the tested bacterial strains according to the guidelines of the Clinical and Laboratory Standards Institute (22). Briefly, the bacterial suspensions were prepared by suspending bacterial cultures grown for 18 h in sterile normal saline (0.85% NaCl [wt/vol]; HiMedia). The turbidity of the bacterial suspensions was adjusted to a 0.5 McFarland standard (equivalent to 1.5×10^8 CFU/ml). Cu_2O-NPs and bulk copper stock solutions were prepared in Milli-Q water, and 2-fold serial dilutions were prepared in Mueller-Hinton broth (MHB) (HiMedia) in a 100-μl volume in 96-well U-bottom microtiter plates (Tarson, Mumbai, India). The above-mentioned bacterial suspension was further diluted in MHB, and a 100-μl volume of this diluted inoculum was added to each well of the plate, resulting in the final inoculum of 5×10^5 CFU/ml in the well, and the final concentration of Cu_2O-NPs ranged from 10 to 10,000 μg/ml. The plates were incubated at 37°C for 18 h and were visually read for the absence or presence of turbidity. Similarly, the MICs of vancomycin and daptomycin were evaluated. The MIC of vancomycin-BODIPY (dipyrromethene boron difluoride [4,4-difluoro-4-bora-3*a*,4*a*-diaza-*s*-indacene] fluorescent dye; Invitrogen, Carlsbad, CA, USA) was evaluated only for the St1745 (hVISA) strain. The MIC was defined as the minimum concentration of the compound that showed no bacterial turbidity.

Biofilm susceptibility assay. The biofilms of selected *S. aureus* isolates (Mu3, Mu50, ATCC 29213, and clinical isolates [St1745 and B10760]) were prepared in 96-well flat-bottom polystyrene microtiter plates (Tarson), using a previously described method (23). Wells with and without culture were used as positive and negative controls, respectively. The bacterial suspensions were prepared from the overnight grown culture, and the turbidity of the suspension was adjusted to an optical density at 610 nm (OD_{610}) of 0.7 (≈1×10^9 CFU/ml). Two-fold serial dilutions of Cu_2O-NPs were prepared in 100-μl volumes in BHIB in the wells of 96-well flat-bottom microtiter plates. Forty microliters of fresh BHIB was added to each well, followed by the addition of 60 μl of the above-mentioned bacterial suspension. This resulted in the final inoculum of 6×10^7 CFU/ml in each well; the final concentrations of the compounds ranged from 78 to 10,000 μg/ml. The plate was incubated for 18 h at 37°C. After incubation, the planktonic cells were removed from each well by washing with phosphate-buffered saline (PBS) (HiMedia). The biofilms were fixed with methanol for 15 to 30 min, stained with 0.1% (wt/vol) crystal violet (Sigma Chemical Co., St. Louis, MO, USA) for 10 min, and rinsed thoroughly with water until the negative-control wells appeared colorless. Biofilm formation was quantified by the addition of 200 μl of 95% ethanol to the crystal violet-stained wells, and the absorbance was recorded at 595 nm (A_{595}) using a microplate reader (Spectra easy microplate reader; Inverness Medicals, India).

Studies on mechanism of action of Cu_2O-NPs. (i) Leakage assay and protein estimation. Leakage of 260- and 280-nm-absorbing compounds was determined spectrophotometrically (24). Briefly, the bacterial cells (all tested strains) were grown overnight in 100 ml of MHB at 37°C, washed, and resuspended in 50 mM sodium phosphate buffer (pH 7.1). The turbidity of the suspension was adjusted to an OD_{610} of 0.7 (≈1×10^9 CFU/ml). Cu_2O-NPs were added at 5,000 μg/ml to the bacterial suspension (≈1×10^9 CFU/ml) and incubated for 120 min at 37°C. For complete release of 260- and 280-nm-absorbing compounds, the bacterial suspension was treated with cetyl trimethylammonium bromide (CTAB) (10 μg/ml) at 37°C for 120 min, followed by sonication, and this served as a positive control. Cell supernatants were obtained by centrifugation (10,000 × *g* for 10 min). The absorbance of cell supernatant at 260 and 280 nm was determined using a spectrophotometer (Specgene; Tachne). Background leakage was determined in bacterial suspensions without nanoparticles (negative control). The extent of leakage of 260- and 280-nm-absorbing compounds was expressed as a percentage of the positive control (suspension treated with CTAB) measured in supernatants. Protein in the leaked supernatants was estimated by the method of Lowry et al. (25).

(ii) PI uptake assay. Propidium iodide (PI) uptake was assayed by flow cytometric analysis following the previously published protocol (26). Briefly, a clinical isolate of hVISA (St1745) was cultured in BHIB with aeration at 37°C for 24 h of incubation. Cu_2O-NPs at the concentration of 2× MIC were added to the cells, and the cells were incubated for 0, 8, and 24 h. Untreated bacterial cultures were used as controls. The cells were harvested by centrifugation at 8,000 rpm for 10 min at 25°C, washed twice with 50 mM PBS buffer (pH 7.0), and subsequently resuspended in PBS to obtain a final concentration of 10^8 CFU/ml. Bacterial suspensions were then incubated with 50 μg/ml of PI (Sigma Chemical Co.) in the dark for 15 min. Further, the samples were analyzed at the FL-1 channel (488 nm; blue argon laser) on a flow cytometer (Canto II, Becton Dickinson, San Jose, CA, USA) using FlowJo software.

(iii) EtBr uptake assay. The disruptive effect of Cu_2O-NPs was assessed on a clinical isolate of hVISA (St1745) by using Cu_2O-mediated ethidium bromide (EtBr) uptake. One ml of 1.0×10^6 CFU/ml cell suspension of hVISA (St1745) in PBS was incubated with 0.5×, 1×, and 2× MIC of Cu_2O-NPs at 37°C for 2 h with shaking. EtBr (100 μM; a 1 mg/ml solution) was added to all different concentrations of Cu_2O-NP-treated

bacterial cells and incubated at room temperature for 15 min. Cells with EtBr and no Cu_2O-NPs served as negative controls. Cells were washed and resuspended in PBS, and 1 drop of each suspension was examined under a fluorescence microscope at ×100 magnification (Olympus, Tokyo, Japan) for red fluorescence.

(iv) Salt tolerance assay. The ability of bacterial cells (St1745) treated with mixtures of Cu_2O-NPs and sodium chloride to grow on Mueller-Hinton agar (MHA) (HiMedia) was investigated according to the previously published protocol (27) with slight modifications. Suspensions of bacteria (10^6 CFU/ml) were prepared in MHB (HiMedia) and treated with 0.5× MICs, 1× MICs, and 2× MICs of Cu_2O-NPs and 1% dimethyl sulfoxide (DMSO). In other groups, each concentration was combined with 7.5% NaCl, and the control was set up without Cu_2O-NPs. The test tubes were incubated in a shaking incubator at 37°C, and samples were removed at intervals, serially diluted, and plated on MHA. After 24 h of incubation, the numbers of colonies (CFU/ml) were counted on plates and compared with those of the control.

(v) Binding of fluorescently labeled vancomycin to *S. aureus* St1745 biofilm. Biofilms were formed on 96-well flat-bottomed polystyrene plates as described above. After two washes with PBS, the biofilms were incubated with 50 μl of 40 mM vancomycin-BODIPY dissolved in PBS for 0, 5, 15, 30, and 60 min at room temperature. After two washes with PBS, the fluorescence derived from vancomycin-BODIPY was measured with a microplate reader (Synergy HT; BioTek, USA) at excitation and emission wavelengths of 485 and 535 nm, respectively. After a 60-min incubation, the biofilms were washed with PBS to remove unbound vancomycin-BODIPY and resuspended. The localization of vancomycin-BODIPY was analyzed by fluorescence microscopy using a green fluorescent protein filter (Olympus).

Toxicity assessment. The toxicity of Cu_2O-NPs was determined by a hemolysis assay as described previously (28) with a few modifications. The modifications were as follows: we used different concentrations of nanoparticles and red blood cells (RBCs) instead of whole blood. Briefly, blood samples were collected from healthy volunteers and stored in EDTA Vacutainer tubes. Whole blood (5 ml) was added to 10 ml of PBS and centrifuged at 10,016 × *g* for 10 min to separate the RBCs. The RBCs were then washed five times with 10 ml of PBS and diluted to 50 ml with PBS. To test the hemolytic activity of Cu_2O-NPs, 0.2 ml of the diluted RBC suspension was added to 0.8 ml of the nanoparticle solution at different concentrations ranging from 625 to 10,000 μg/ml. Triton X-100 was used as a positive control, and a sample without treatment with nanoparticles was used as a negative control. All samples were placed on a rocking shaker at 37°C for 3 h. After incubation, the samples were centrifuged at 10,016 × *g* for 3 min. The hemoglobin absorbance in the supernatant was measured at 570 nm.

Statistical analysis. All the experiments were carried out in triplicate on different occasions. The data were analyzed by Mann-Whitney tests and one-way analysis of variance (ANOVA) for comparison of multiple means followed by Tukey's test using GraphPad Prism 5 (GraphPad Software, Inc., San Diego, CA). The chosen level of significance for all statistical tests was a P value of <0.05.

RESULTS

Structural and morphological characterizations. The powder X-ray diffraction (PXRD) pattern of the Cu_2O-NPs is given in Fig. 1. There were four clear peaks. All of them were perfectly indexed to a single phase of crystalline Cu_2O (Joint Committee on Powder Diffraction Standards [JCPDS] no. 78-2076), not only in their peak position but also to their relative intensity, and the results presented here coincide well with the literature values. The peaks with 2θ values were 37.7402, 43.6758, 62.8232, and 75.0440 corresponding to the crystal planes of (111), (200), (220), and (311) of crystalline Cu_2O, respectively. From the PXRD data, the average crystallite size was calculated

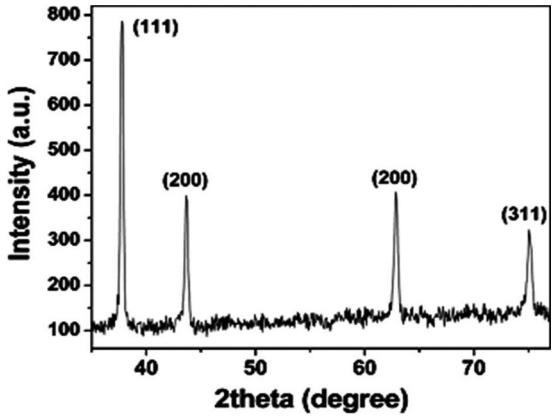

FIG 1 The powder X-ray diffraction (PXRD) pattern of the Cu_2O nanoparticles. a.u., arbitrary units.

to be between 21 and 30 nm for different samples using the Scherrer equation. The morphology and size of the product were studied by electron microscopy. The field emission scanning electron microscopy (FESEM) images (Fig. 2) clearly showed the general morphology of the synthesized Cu_2O-NPs used in this work. The majority of the Cu_2O-NPs had octahedral structures with sizes ranging from 100 to 150 nm. Since the average crystallite size of the Cu_2O particles was between 21 and 30 nm, they fell under the category of nanoparticles.

MICs and minimum biofilm inhibitory concentrations. Cu_2O-NPs were active against hVISA/VISA. The MICs of Cu_2O-NPs were 1,250, 2,500, 625, and 1,250 and 1,250 μg/ml against hVISA (Mu3, standard strain), VISA (Mu50, standard strain), *S. aureus* 29213, and two clinical isolates of hVISA, respectively (Table 1). Cu_2O-NPs effectively inhibited the formation of hVISA/VISA biofilms with 80% minimum biofilm inhibition concentrations (MBICs) ranging from 2,500 μg/ml to 10,000 μg/ml (Fig. 3). The detailed MIC profiles of vancomycin and daptomycin against all tested strains are given in Table 1. Furthermore, the MIC of vancomycin-BODIPY against the daptomycin-nonsusceptible strain of hVISA (St1745) was determined (3 μg/ml) and remained unchanged with BODIPY labeling. In the present study, St1745 (hVISA) was selected for further studies on activities of Cu_2O-NPs.

Studies on mechanism of action of Cu_2O-NPs. (i) Leakage assays. The membrane leakage assays illustrated the cytoplasmic membrane damage for all tested strains of hVISA. The amounts of 260- and 280-nm-absorbing material in *S. aureus* supernatants exposed to Cu_2O-NPs at 90 min and 120 min were observed. Bacterial cells with exposure to CTAB (100% cell lysis) and without exposure to either Cu_2O-NPs or CTAB served as the positive and negative controls, respectively. The leakage of proteins from bacterial cells was 69.9% at both 90 min and 120 min when exposed to Cu_2O-NPs and 39.8% in negative controls compared to that in positive controls. The leakage of proteins from cell membranes was higher in CTAB (positive control) and the Cu_2O-NP-treated strain Mu3 and clinical isolates of hVISA than in the Mu50 (VISA) strain ($P < 0.001$) (Fig. 4).

(ii) PI uptake assay. hVISA (St1745) cells treated with 2× MIC of Cu_2O-NPs for 0, 8, and 24 h resulted in the identification of two subpopulations (PI-positive and PI-negative cells) by flow cytom-

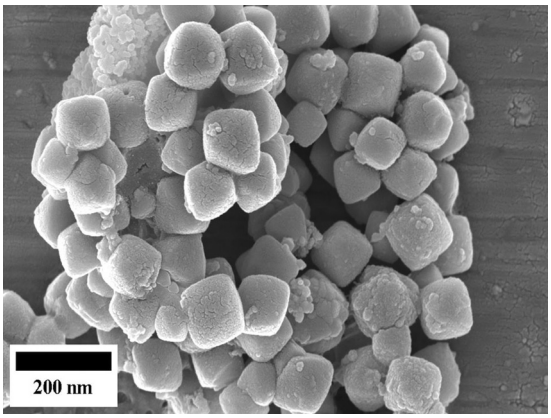

FIG 2 Field emission scanning electron microscopy (FESEM) images of the synthesized Cu_2O nanoparticles.

etry analysis. The PI-positive and PI-negative cells represented dead and viable cells, respectively. The effect of Cu_2O-NPs against hVISA cells was observed to be time dependent. After 4 h of incubation, the rate of dead cells was 92.6% ± 2.4%, and this increased to 94.1% within 8 h in the case of the clinical hVISA isolate (P = 0.0001) (Fig. 5).

(iii) Loss of salt tolerance. A reduction in the viability of hVISA (St1745) cells on agar medium with 7.5% NaCl in the presence of Cu_2O-NPs at the MIC and 2× MIC was observed. This treatment reduced the salt tolerance ability of the bacteria by about 3.6-fold in the clinical isolate of hVISA after both 12 and 24 h of treatment (Fig. 6).

(iv) EtBr uptake. Very few non-Cu_2O-NP-treated clinical isolates of hVISA (St1745) cells stained with EtBr showed fluorescence. However, Cu_2O-NP-treated cells exhibited increased uptake of EtBr, which was proportional to the Cu_2O-NP concentration. Cu_2O-NPs at 2× MIC resulted in complete and homogeneous staining of cells (Fig. 7).

(v) Binding of fluorescently labeled vancomycin to hVISA (St1745) biofilm. We analyzed the localization of vancomycin-BODIPY (fluorescently labeled vancomycin) in hVISA and VISA biofilms. BODIPY labeling seemed to have no effect on the activity of vancomycin, since the MIC of the hVISA strain (St1745) remained unchanged (3 μg/ml) (Table 1). After treatment of biofilm cells with Cu_2O-NPs (2× MIC), the fluorescence derived from vancomycin-BODIPY was measured at different incubation times. Significant (P = 0.0001) reductions in fluorescence were observed in the treated *S. aureus* strains (ATCC 29213, Mu3, Mu50, St1745, and B10760 isolates) compared to those in the respective untreated strains at 60 min; the reductions were 39.1%, 21.38%, 38.77%, 28.3%, and 25.9%, respectively (Fig. 8). The biofilm was suspended in PBS and observed under a fluorescence microscope. Fluorescence was observed at the surface of virtually every cell. It was also observed at the level of the septa in a few cells (Fig. 9).

(vi) Toxicity assessment. The concentration of hemoglobin present in the samples was calculated from the absorbance values. No cytotoxicity was observed at 625 to 10,000 μg/ml concentrations of Cu_2O-NPs (Fig. 10).

DISCUSSION

In the present study, Cu_2O-NPs were synthesized according to the solution phase method. The structural and morphological characterizations of Cu_2O-NPs and their antibiofilm behavior were investigated. Cu_2O-NPs showed bacterial membrane-damaging potential and appeared to be the main cause of the bactericidal activity against *S. aureus* strains with reduced vancomycin susceptibility. The identification of the surface morphology, the particle size, and the defined elemental composition of nanoparticulate Cu_2O are required for its potential application as an antimicrobial agent. The FESEM image clearly showed the general morphology of the synthesized Cu_2O-NPs, and the majority of the Cu_2O-NPs were in the range of 100 to 150 nm. Therefore, it was estimated that most of the nanoparticulates generated by the solution phase technology were indeed Cu_2O.

Previously, it had been reported that copper (Cu)-containing nanoparticles (Cu metal, Cu, CuO) caused cell membrane damage, depending on both the chemical composition (metal versus oxide) and surface area (21). Cu_2O-NPs are considered effective in killing a range of bacterial pathogens involved in hospital-acquired infections. However, higher concentrations of Cu_2O-NPs than of silver nanoparticles (Ag NPs) and copper nanoparticles (Cu NPs) are required to achieve a bactericidal effect (4). It was suggested that the reduced amount (between 3- and 20-fold) of negatively charged peptidoglycans might make Gram-negative bacteria less susceptible to positively charged antimicrobials (29). Previous work on nanoparticles revealed that Ag and Cu nanoparticles released Ag^+ and Cu^{2+} ions having antiviral capabilities by altering local pH and conductivity along with the liberation of metal ions that had the ability to inactivate or kill viruses (4).

In the present study, the *in vitro* experiments with Cu_2O-NPs synthesized in our laboratory revealed that these nanoparticles had significant antibacterial activity against hVISA compared to that of bulk copper. Our finding is concordant with that of a previous study (4). Staphylococci are responsible for a large percentage of catheter-related infections, and, like other pathogens, they tend to form a multilayered community of sessile bacterial cells known as a biofilm on medical implants and damaged tissues rather than living as free planktonic cells (30). However, reports

TABLE 1 MICs of Cu_2O nanoparticles, vancomycin, and daptomycin against *Staphylococcus aureus*

Sample no.	Microorganism[a]	MIC (μg/ml)[b]				
		Cu_2O-NPs	Bulk copper	Van	Dapto	Van-BODIPY
1	Mu3 (hVISA)	1,250	2,500	2	1	ND
2	Mu50 (VISA)	2,500	5,000	8	1	ND
3	Clinical isolate of hVISA (n = 2)					
	St1745	1,250	2,500	3	2 (NS)	3
	B10760	1,250	2,500	3	1	ND
4	*S. aureus* ATCC 29213	625	2,500	1.5	0.5	ND

[a] hVISA, heterogeneous vancomycin-intermediate *S. aureus*; VISA, vancomycin-intermediate *S. aureus*.
[b] Van, vancomycin; Dapto, daptomycin; Van-BODIPY, vancomycin-BODIPY (dipyrromethene boron difluoride [4,4-difluoro-4-bora-3*a*,4*a*-diaza-*s*-indacene] fluorescent dye); NS, nonsusceptible; ND, not done.

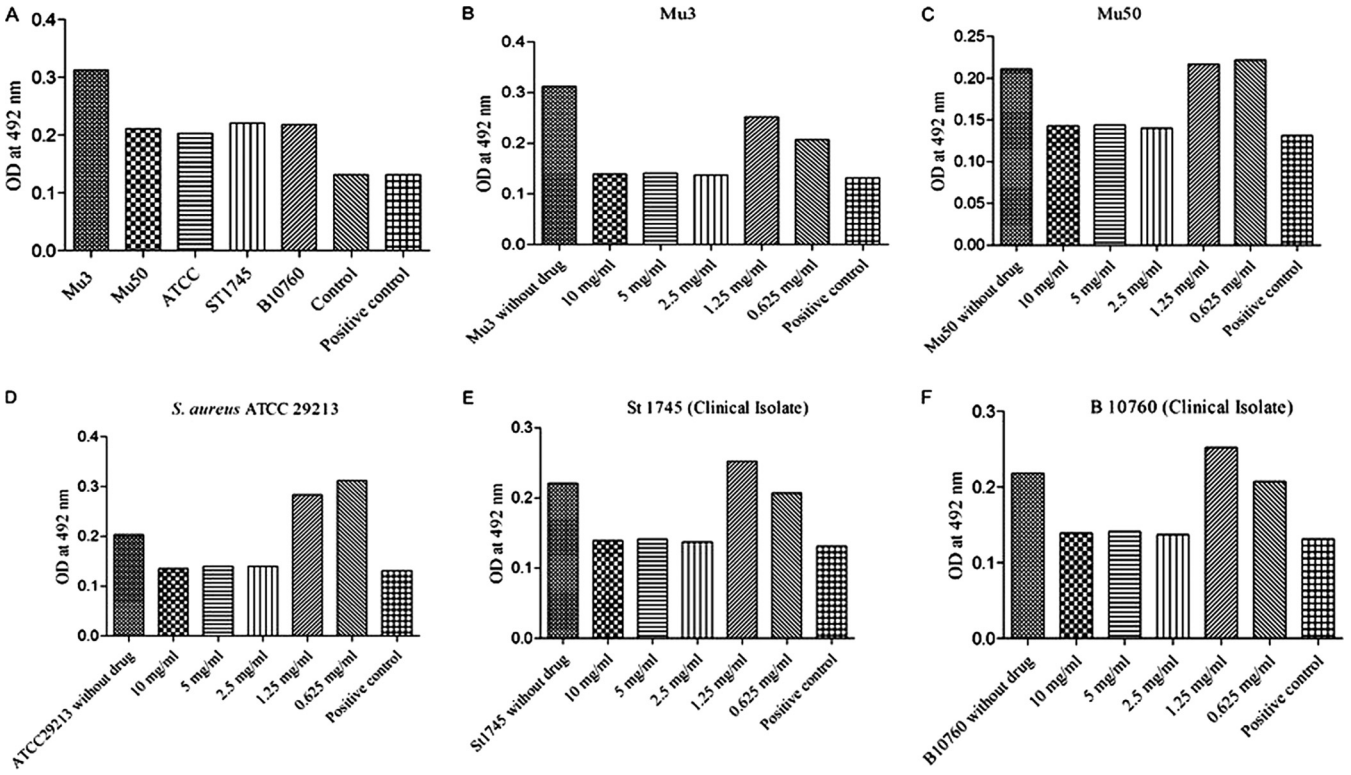

FIG 3 (A) Biofilm formation by *S. aureus* strains. (B to F) Biofilm inhibitory concentration of Cu_2O-NPs against *Staphylococcus aureus* strains Mu3, Mu50, ATCC 29213, St1745, and B10760, respectively.

are available in which Cu_2O was shown to effectively inhibit the staphylococcal bacterial pathogens (31), but the antibiofilm activity of Cu_2O-NPs against hVISA/VISA-type resistant strains has not yet been reported. In addition, patients infected with hVISA/VISA face major therapeutic challenges because of vancomycin treatment failure (32). Such infections are difficult to treat due to their inherent antibiotic resistance (8). In the present study, the MBIC of Cu_2O-NPs was 2-fold higher than the MIC for *S. aureus*. However, lower antibacterial activity of Cu_2O-NPs was found against the Mu50 (VISA) bacteria. This might be attributable to the presence of the thick cell wall of Mu50 (VISA) compared to that of Mu3 (hVISA) (3). Studies using atomic force microscopy and transmission electron microscopy with aerogel-generated nano-magnesium oxide against *E. coli* showed that the cell wall of this bacterium was extensively damaged, allowing the contents to leak out and nanoparticles to gain entry (14, 33). Likewise, Ag NPs have been shown to attach to the microbial cell surface and penetrate inside, where intracellular targets, including respiratory enzymes, were disrupted (34).

However, the exact mechanism of action of Cu_2O-NPs against hVISA/VISA isolates has not been reported so far. We investigated

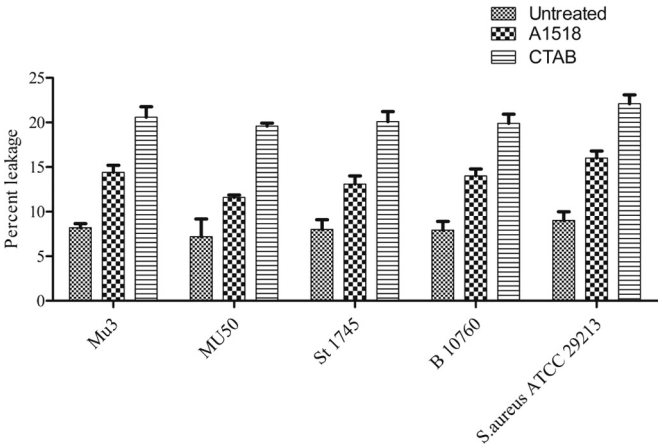

FIG 4 Percent leakage of protein estimated by the method of Lowry et al. (25) in Mu3 (hVISA) and Mu50 (VISA) strains treated with Cu_2O-NPs; CTAB-treated cells served as the positive control.

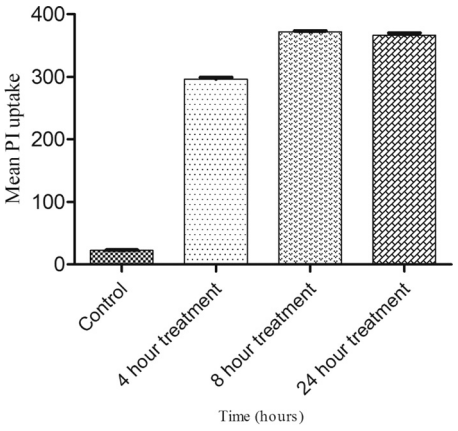

FIG 5 Mean fluorescence intensity of propidium iodide uptake in St1745 (hVISA) cells treated with 2× MIC of Cu_2O-NPs.

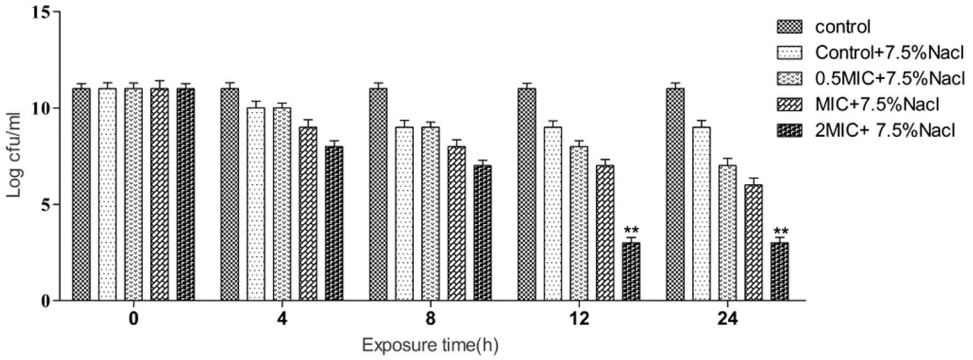

FIG 6 The ability of St1745 (hVISA) to form colonies on Mueller-Hinton agar (MHA) supplemented with 7.5% NaCl after treatment with 0.5× MIC, 1× MIC, and 2× MIC of Cu_2O-NPs. **, $P < 0.001$.

the potential membrane damage due to Cu_2O-NPs by measuring the leakage of bacterial cell contents, EtBr uptake, salt tolerance, and finally the PI uptake by flow cytometry. The leakage of cytosolic constituents (260- and 280-nm-absorbing materials) from *S. aureus* cells in the presence of 50 mg/liter Cu_2O-NPs over a period of 2 h was significantly higher than the background levels (Fig. 4). The leakage of cytosolic constituents indicated that Cu_2O-NPs altered the cell membrane structure, resulting in the disruption of the permeability barrier of microbial membrane structures, which is in concordance with the previous study (14).

Further, we examined membrane integrity by a salt tolerance assay. *S. aureus* is known for its ability to survive in the presence of high salt concentrations due to accumulation of osmoprotectants, such as choline and L-proline (35, 36). Cu_2O-NPs were found to reduce the tolerance of hVISA/VISA to low osmotic pressure (Fig. 6). The MIC and 2× MIC ($P = 0.001$) of Cu_2O may alter the permeability and affect the ability of the membrane to osmoregulate cells adequately or to exclude toxic material. A previous study reported that tea tree and *Origanum vulgare* essential oils and lichen *Usnea subfloridana*-derived usnic

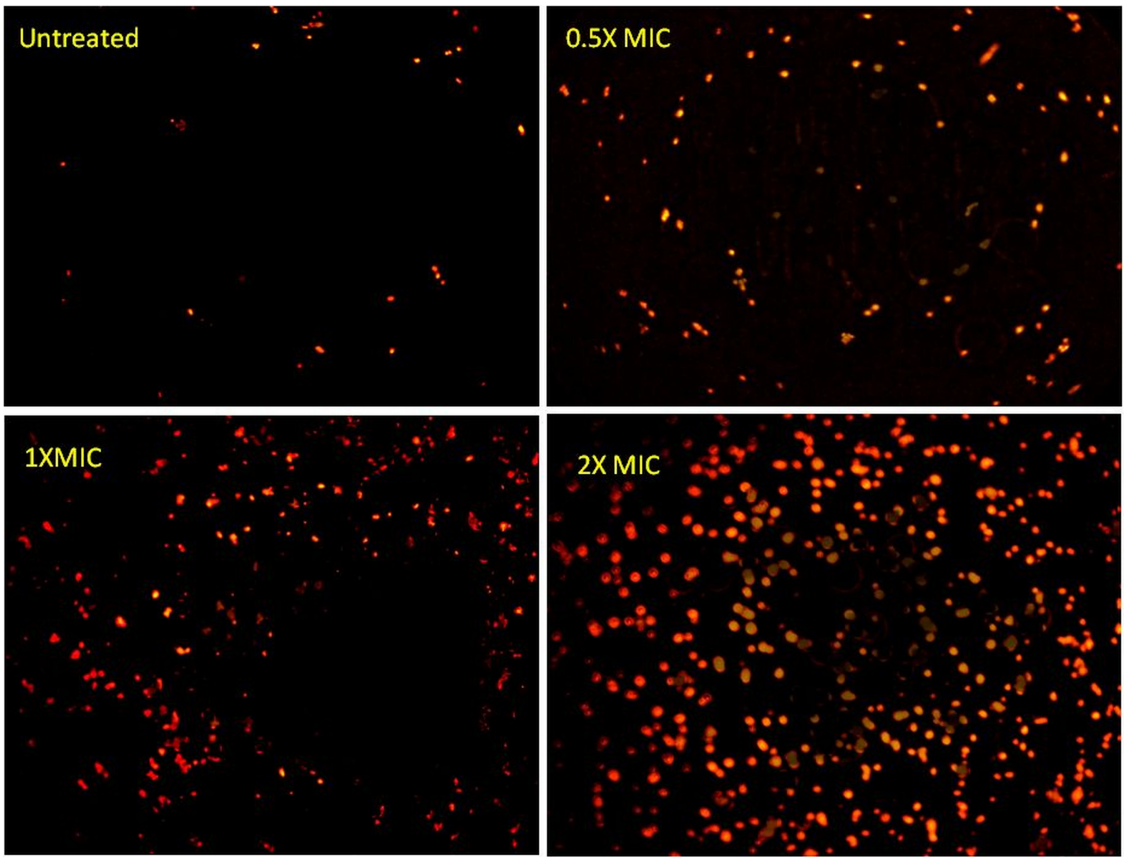

FIG 7 Ethidium bromide uptake following exposure to 0, 0.5×, 1×, and 2× MICs of Cu_2O-NPs as assessed by fluorescence microscopy at ×100 magnification (Olympus, Tokyo, Japan).

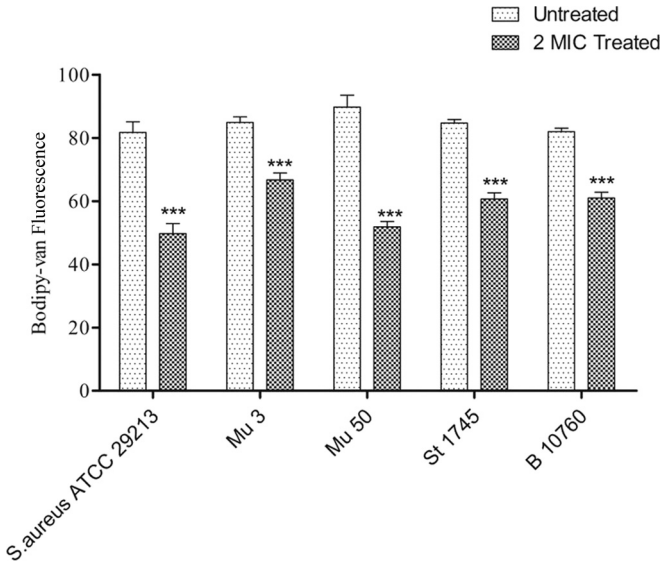

FIG 8 Relative vancomycin binding to hVISA (strain St1745) (means ± standard deviations) in the presence and absence of 2× MIC of Cu_2O-NPs. ***, $P < 0.0001$.

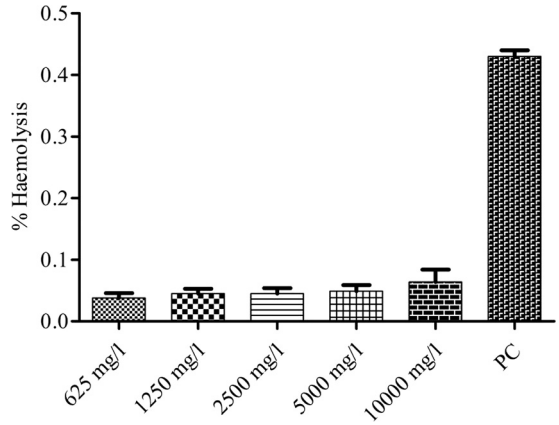

FIG 10 Percent hemolysis values of Cu_2O-NPs at 625 to 10,000 mg/liter for human red blood cells (RBCs). PC, positive control (Triton X-100-treated RBCs).

acid caused significant loss of salt tolerance through membrane damage in bacteria (37).

In the present study, a significant ($P = 0.0001$) increase in PI uptake was observed in the Cu_2O-NP-treated hVISA (St1745) cells within 4 h (92.6%), which further increased to 94.1% within

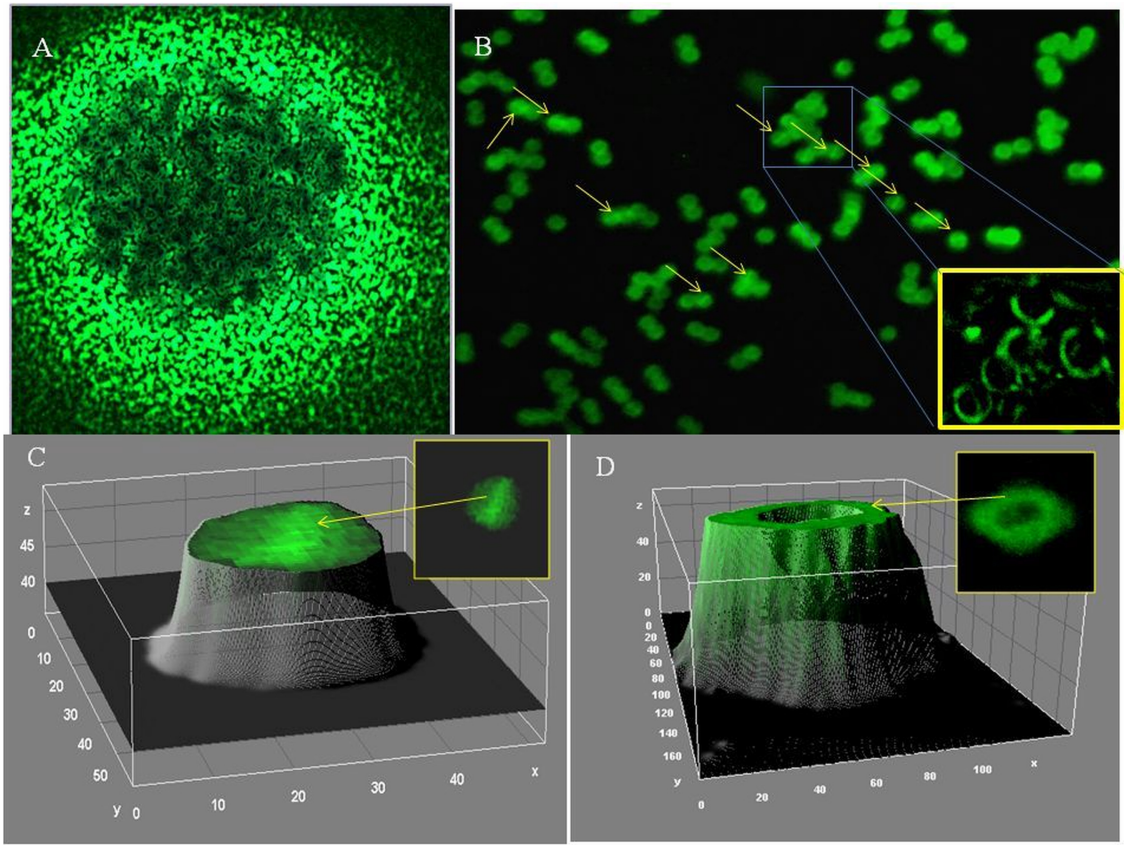

FIG 9 (A) hVISA (strain St1745) biofilms treated with 2× MIC of Cu_2O-NPs for 1 h and then treated with 3 mg/liter vancomycin-BODIPY for 15 min (fluorescence microscopy at ×40 magnification). (B) Localization analysis of vancomycin-BODIPY after a 15-min incubation; the biofilms resuspended in PBS were observed by fluorescence microscopy at ×100 magnification. Arrows, division of septa of the cells (inset, enlargement of boxed area). (C) Three-dimensional (3D) view of vancomycin binding to the septum of hVISA cells during cell division. (D) 3D view of vancomycin binding to only the cell wall of *S. aureus* during cell division.

8 h (Fig. 5). This rapid increase in PI uptake confirms that the antibiofilm activity of Cu_2O-NPs was due to cell membrane disruption. Because of its large size and negative charge, PI cannot pass through the intact membranes of bacteria (38).

Bacterial cells damaged by Cu_2O-NPs were further visualized by EtBr uptake under a fluorescence microscope. It has been reported that EtBr can enter and intercalate within the DNA of compromised bacterial cells with high fluorescence (39). Therefore, the present experiment was designed to assess Cu_2O-NP-mediated uptake of EtBr in cells exposed to Cu_2O as a measurement of cell integrity. Microscopic images revealed enhanced uptake of EtBr by Cu_2O-exposed cells that was proportional to the Cu_2O-NP concentration (Fig. 7). An increase in the penetration of cells by EtBr just minutes after the addition of Cu_2O indicates that this compound damages the bacterial cell membrane rapidly. Further, a reduction in vancomycin-BODIPY fluorescence was observed in Cu_2O-NP-treated cells compared to that in untreated cells (Fig. 8), suggesting that Cu_2O-NPs might also affect cell wall synthesis. Moreover, the binding of vancomycin-BODIPY with the septum of a bacterium within 15 min of vancomycin-BODIPY exposure indicates penetration of vancomycin toward the septum (Fig. 9A to D). Similar findings were reported with commercially purchased nisin A and lacticin Q isolated from *Lactococcus lactis* against methicillin-resistant *S. aureus* (MRSA) (40). It is most likely that Cu_2O-NP exposure also caused a significant reduction in cell wall thickness, as evidenced by a reduction in vancomycin-BODIPY fluorescence. A similar relationship was reported earlier between cell wall thickness and exposure to nafcillin and the vancomycin and ceftaroline combination against hVISA/VISA (41). Our observations have led us to hypothesize that the disruption of the cell membrane and the reduction in vancomycin-BODIPY fluorescence is due to cell wall thinning that prevents vancomycin sequestration and improves vancomycin penetration into the septa of dividing cells. The division of the septum is the active site of cell wall biosynthesis in *S. aureus*, and any antimicrobial agent that inhibits the late steps of cell wall biosynthesis must have access to lipid II at the septum (42). However, further studies are required to explore the exact mechanisms of cell wall thinning by Cu_2O-NPs in hVISA. The toxicity assessment of Cu_2O-NPs by a hemolysis assay showed no cytotoxicity at different concentrations (Fig. 10). However, to substantiate this observation, *in vivo* toxicity assessment is warranted.

Our results indicate that the A1518 Cu_2O-NPs effectively inhibited the growth of hVISA and VISA strains and also reduced their ability to form biofilms. To our knowledge, this is the first report to provide evidence that Cu_2O-NPs have a membrane-damaging potential in *S. aureus* and can be used as an effective antibiofilm agent against *S. aureus*. However, this study does have some limitations: (i) there might be an alternative mechanism(s) for the bacterial cell deaths, e.g., interactions of Cu_2O-NPs with biological macromolecules such as enzymes and DNA; and (ii) we did not perform toxicity studies on human cell lines and in animal models.

In conclusion, it is noteworthy that the synthesis of Cu_2O-NPs by the solution phase method is simple, economical, and safe. The probable mode of action of Cu_2O-NPs is disruption of bacterial cell membranes. These nanoparticles can be used as a chemical biocide for destroying drug-resistant staphylococci and their biofilms. Further, Cu_2O-NPs have the potential to be used in medical and household devices as effective antibiofilm agents since they showed no toxicity in an *in vitro* hemolysis assay. However, further *in vitro* and *in vivo* experiments are required before final conclusions can be drawn.

ACKNOWLEDGMENTS

We thank Hiramatsu for providing the Mu3 (hVISA) and Mu50 (VISA) strains.

We acknowledge the financial support provided by SGPGIMS through intramural grant 2013-30-IMP-EXP/177. Avinash Singh and Sonali Khanduja acknowledge the financial assistance received from the Indian Council of Medical Research (ICMR), Government of India, New Delhi, through senior research fellowship grants 80/675/10-ECD-I and 80/829/2003-ECD-I, respectively. Satyendra K. Singh also acknowledges support from the CSIR, Government of India, through junior research fellowship grant CSIR JRF-09/590(0147)/2010-EMR-1.

REFERENCES

1. **Yarwood JM, Bartels DJ, Volper EM, Greenberg EP.** 2004. Quorum sensing in *Staphylococcus aureus* biofilms. J Bacteriol **186:**1838–1850. http://dx.doi.org/10.1128/JB.186.6.1838-1850.2004.
2. **Faúndez G, Troncoso M, Navarrete P, Figueroa G.** 2004. Antimicrobial activity of copper surfaces against suspensions of *Salmonella enterica* and *Campylobacter jejuni*. BMC Microbiol **4:**19. http://dx.doi.org/10.1186/1471-2180-4-19.
3. **Howden BP, Johnson PD, Ward PB, Stinear TP, Davies JK.** 2006. Isolates with low-level vancomycin resistance associated with persistent methicillin-resistant *Staphylococcus aureus* bacteremia. Antimicrob Agents Chemother **50:**3039–3047. http://dx.doi.org/10.1128/AAC.00422-06.
4. **Ren G, Hu D, Cheng EW, Vargas-Reus MA, Reip P, Allaker RP.** 2009. Characterisation of copper oxide nanoparticles for antimicrobial applications. Int J Antimicrob Agents **33:**587–590. http://dx.doi.org/10.1016/j.ijantimicag.2008.12.004.
5. **Howden BP, Ward PB, Charles PG, Korman TM, Fuller A, du Cros P, Grabsch EA, Roberts SA, Robson J, Read K, Bak N, Hurley J, Johnson PD, Morris AJ, Mayall BC, Grayson ML.** 2004. Treatment outcomes for serious infections caused by methicillin-resistant *Staphylococcus aureus* with reduced vancomycin susceptibility. Clin Infect Dis **38:**521–528. http://dx.doi.org/10.1086/381202.
6. **Vuong C, Saenz HL, Gotz F, Otto M.** 2000. Impact of the agr quorum-sensing system on adherence to polystyrene in *Staphylococcus aureus*. J Infect Dis **182:**1688–1693. http://dx.doi.org/10.1086/317606.
7. **Sakoulas G, Eliopoulos GM, Moellering RC, Jr, Novick RP, Venkataraman L, Wennersten C, DeGirolami PC, Schwaber MJ, Gold HS.** 2003. *Staphylococcus aureus* accessory gene regulator (*agr*) group II: is there a relationship to the development of intermediate-level glycopeptide resistance? J Infect Dis **187:**929–938. http://dx.doi.org/10.1086/368128.
8. **Dunne WM, Jr.** 2002. Bacterial adhesion: seen any good biofilms lately? Clin Microbiol Rev **15:**155–166. http://dx.doi.org/10.1128/CMR.15.2.155-166.2002.
9. **Bagga B, Reddy AK, Garg P.** 2010. Decreased susceptibility to quinolones in methicillin-resistant *Staphylococcus aureus* isolated from ocular infections at a tertiary eye care centre. Br J Ophthalmol **94:**1407–1408. http://dx.doi.org/10.1136/bjo.2010.179747.
10. **Howden BP, Davies JK, Johnson PD, Stinear TP, Grayson ML.** 2010. Reduced vancomycin susceptibility in *Staphylococcus aureus*, including vancomycin-intermediate and heterogeneous vancomycin-intermediate strains: resistance mechanisms, laboratory detection, and clinical implications. Clin Microbiol Rev **23:**99–139. http://dx.doi.org/10.1128/CMR.00042-09.
11. **Singh A, Prasad KN, Misra R, Rahman M, Singh SK, Rai RP, Tripathi A, Srivastava JK.** 29 May 2015. Increasing trend of heterogeneous vancomycin intermediate *Staphylococcus aureus* in a tertiary care center of northern India. Microb Drug Resist http://online.liebertpub.com/doi/abs/10.1089/mdr.2015.0004.
12. **Maor Y, Rahav G, Belausov N, Ben-David D, Smollan G, Keller N.** 2007. Prevalence and characteristics of heteroresistant vancomycin-intermediate *Staphylococcus aureus* bacteremia in a tertiary care center. J Clin Microbiol **45:**1511–1514. http://dx.doi.org/10.1128/JCM.01262-06.
13. **Chen J, Han CM, Lin XW, Tang ZJ, Su SJ.** 2006. Effect of silver nanoparticle dressing on second degree burn wound. Zhonghua Wai Ke Za Zhi **44:**50–52. (In Chinese.)

14. **Stoimenov PK, Klinger RL, Marchin GLM, Klabunde KJ.** 2002. Metal oxide nanoparticles as bactericidal agents. Langmuir **18:**6679–6686. http://dx.doi.org/10.1021/la0202374.
15. **Usman MS, El Zowalaty ME, Shameli K, Zainuddin N, Salama M, Ibrahim NA.** 2013. Synthesis, characterization, and antimicrobial properties of copper nanoparticles. Int J Nanomed **8:**4467–4479. http://dx.doi.org/10.2147/IJN.S50837.
16. **Gopalkrishnan K, Ramesh C, Ragunathan V, Thamilselvan M.** 2012. Antibacterial activity of Cu_2O nanoparticles on *E. coli* synthesized from *Tridax procumbens* leaf extract and surface coating with polyaniline. Dig J Nanomater Biostruct **7:**833–839.
17. **Huang LN, Wang HT, Wang ZB, Mitra A.** 2002. Cuprite nanowires by electrodeposition from lyotropic reverse hexagonal liquid crystalline phase. Chem Mater **14:**876–880. http://dx.doi.org/10.1021/cm010819r.
18. **Ruparelia JP, Chatterjee AK, Duttagupta SP, Mukherji S.** 2008. Strain specificity in antimicrobial activity of silver and copper nanoparticles. Acta Biomater **4:**707–716. http://dx.doi.org/10.1016/j.actbio.2007.11.006.
19. **Seigfried MJ, Choi KS.** 2005. Directing the architecture of cuprous oxide crystals during electrochemical growth. Angew Chem **117:**3282–3287. http://dx.doi.org/10.1002/ange.200463018.
20. **Asar A, Namdeo SG, Amish GJ.** 2011. Low cost, surfactant less, one pot synthesis of Cu_2O nano-octahedra at room temperature. J Solid State Chem **184:**2209–2214. http://dx.doi.org/10.1016/j.jssc.2011.05.058.
21. **Karlsson HL, Cronholm P, Hedberg Y, Tornberg M, De Battice L, Svedhem S, Wallinder IO.** 2013. Cell membrane damage and protein interaction induced by copper containing nanoparticles—importance of the metal release process. Toxicology **313:**59–69. http://dx.doi.org/10.1016/j.tox.2013.07.012.
22. **Clinical and Laboratory Standards Institute.** 2012. Methods for dilution antimicrobial susceptibility tests for bacteria that grow aerobically, 9th ed. Approved standard M7-A7. Clinical and Laboratory Standards Institute, Wayne, PA.
23. **Wei GX, Campagna AN, Bobek LA.** 2006. Effect of MUC7 peptides on the growth of bacteria and on *Streptococcus mutans* biofilm. J Antimicrob Chemother **57:**1100–1109. http://dx.doi.org/10.1093/jac/dkl120.
24. **Cox SD, Mann CM, Markham JL, Gustafson JE, Warmington JR, Wyllie SG.** 2001. Determining the antimicrobial actions of tea tree oil. Molecules **6:**87–91. http://dx.doi.org/10.3390/60100087.
25. **Lowry OH, Rosebrough NJ, Farr AL, Randall RJ.** 1951. Protein measurement with the Folin phenol reagent. J Biol Chem **193:**265–275.
26. **Wiczling P, Krzyzanski W.** 2008. Flow cytometric assessment of homeostatic aging of reticulocytes in rats. Exp Hematol **36:**119–127. http://dx.doi.org/10.1016/j.exphem.2007.09.002.
27. **Carson CF, Mee BJ, Riley TV.** 2002. Mechanism of action of *Melaleuca alternifolia* (tea tree) oil on *Staphylococcus aureus* determined by time-kill, lysis, leakage, and salt tolerance assays and electron microscopy. Antimicrob Agents Chemother **46:**1914–1920. http://dx.doi.org/10.1128/AAC.46.6.1914-1920.2002.
28. **Laloy J, Valentine Minet, Alpan L, Mullier F, Beken S, Toussaint O, Lucas S, Dogné J-M.** 2014. Impact of silver nanoparticles on haemolysis, platelet function and coagulation. Nanobiomedicine **1:**4. http://dx.doi.org/10.5772/59346.
29. **Kawahara K, Tsuruda K, Morishita M, Uchida M.** 2000. Antibacterial effect of silver-zeolite on oral bacteria under anaerobic conditions. Dent Mater **16:**452–455. http://dx.doi.org/10.1016/S0109-5641(00)00050-6.
30. **Donlan RM, Murga R, Bell M, Toscano CM, Carr JH, Novicki TJ, Zuckerman C, Corey LC, Miller JM.** 2001. Protocol for detection of biofilms on needleless connectors attached to central venous catheters. J Clin Microbiol **39:**750–753. http://dx.doi.org/10.1128/JCM.39.2.750-753.2001.
31. **Kang S, Pinault M, Pfefferle LD, Elimelech M.** 2007. Single-walled carbon nanotubes exhibit strong antimicrobial activity. Langmuir **23:**8670–8673. http://dx.doi.org/10.1021/la701067r.
32. **Casapao AM, Leonard SN, Davis SL, Lodise TP, Patel N, Goff DA, Laplante KL, Potoski BA, Rybak MJ.** 2013. Clinical outcomes in patients with heterogeneous vancomycin-intermediate *Staphylococcus aureus* (hVISA) bloodstream infection. Antimicrob Agents Chemother **57:**4252–4259. http://dx.doi.org/10.1128/AAC.00380-13.
33. **Sun H, Choy TS, Zhu DR, Yam WC, Fung YS.** 2009. Nano-silver-modified PQC/DNA biosensor for detecting *E. coli* in environmental water. Biosens Bioelectron **24:**1405–1410. http://dx.doi.org/10.1016/j.bios.2008.08.008.
34. **Sondi I, Salopek-Sondi B.** 2004. Silver nanoparticles as antimicrobial agent: a case study on *E. coli* as a model for Gram-negative bacteria. J Colloid Interface Sci **275:**177–182. http://dx.doi.org/10.1016/j.jcis.2004.02.012.
35. **Graham JE, Wilkinson BJ.** 1992. *Staphylococcus aureus* osmoregulation: roles for choline, glycine betaine, proline, and taurine. J Bacteriol **174:**2711–2716.
36. **Hiramatsu K, Cui L, Kuroda M, Ito T.** 2001. The emergence and evolution of methicillin-resistant *Staphylococcus aureus*. Trends Microbiol **9:**486–493. http://dx.doi.org/10.1016/S0966-842X(01)02175-8.
37. **Gupta VK, Verma S, Gupta S, Singh A, Pal A, Srivastava SK, Srivastava PK, Singh SC, Darokar MP.** 2012. Membrane-damaging potential of natural L-(−)-usnic acid in *Staphylococcus aureus*. Eur J Clin Microbiol Infect Dis **31:**3375–3383. http://dx.doi.org/10.1007/s10096-012-1706-7.
38. **Kim S, Lee H, Lee S, Yoon Y, Choi KH.** 2015. Antimicrobial action of oleanolic acid on *Listeria monocytogenes*, *Enterococcus faecium*, and *Enterococcus faecalis*. PLoS One **10:**e0118800. http://dx.doi.org/10.1371/journal.pone.0118800.
39. **Brehm-Stecher BF, Johnson EA.** 2003. Sensitization of *Staphylococcus aureus* and *Escherichia coli* to antibiotics by the sesquiterpenoids nerolidol, farnesol, bisabolol, and apritone. Antimicrob Agents Chemother **47:**3357–3360. http://dx.doi.org/10.1128/AAC.47.10.3357-3360.2003.
40. **Okuda K, Zendo T, Sugimoto S, Iwase T, Tajima A, Yamada S, Sonomoto K, Mizunoe Y.** 2013. Effects of bacteriocins on methicillin-resistant *Staphylococcus aureus* biofilm. Antimicrob Agents Chemother **57:**5572–5579. http://dx.doi.org/10.1128/AAC.00888-13.
41. **Werth BJ, Vidaillac C, Murray KP, Newton KL, Sakoulas G, Nonejuie P, Pogliano J, Rybak MJ.** 2013. Novel combinations of vancomycin plus ceftaroline or oxacillin against methicillin-resistant vancomycin-intermediate *Staphylococcus aureus* (VISA) and heterogeneous VISA. Antimicrob Agents Chemother **57:**2376–2379. http://dx.doi.org/10.1128/AAC.02354-12.
42. **Lunde CS, Rexer CH, Hartouni SR, Axt S, Benton BM.** 2010. Fluorescence microscopy demonstrates enhanced targeting of telavancin to the division septum of *Staphylococcus aureus*. Antimicrob Agents Chemother **54:**2198–2200. http://dx.doi.org/10.1128/AAC.01609-09.